Journal of Sound and Vibration (2002) **253**(4), 735–754
doi:10.1006/jsvi.2000.3508, available online at http://www.idealibrary.com on IDEAL®

DYNAMIC RESPONSE OF WIND-EXCITED BUILDING USING CFD

S. SWADDIWUDHIPONG AND M. S. KHAN

Department of Civil Engineering, National University of Singapore, Blk E1A, #07-03, 1 Engineering Drive 2, Singapore 117576. *E-mails: cvesomsa@nus.edu.sg; z-khan61@hotmail.com*

(*Received* 12 *November* 1999, *and in final form* 27 *November* 2000)

Computational wind engineering as a new branch of computational fluid dynamics (CFD) has been developed recently to evaluate the interaction between wind and buildings numerically. In the present study, a systematic examination of wind effects on tall buildings and flow condition around buildings has been carried out using commercially available CFD software FLUENT 5. Both renormalization group (RNG) k–ε method and large eddy simulation (LES) with the Smagorinsky model are adopted as turbulence models and the results are compared with the wind-tunnel measurements. The weighted amplitude wave superposition (WAWS) method is used to generate atmospheric wind turbulence. The RNG k–ε method can predict the vortex shedding phenomenon well when compared with experiments for uniform flow input, but fails to predict the shedding frequency accurately for fluctuating incoming flow. On the other hand, the LES model shows reasonably good agreement with experiment in predicting vortex-shedding phenomenon for both uniform and fluctuating flows at inlet. Random-vibration based theory is employed for estimating r.m.s. response of tall buildings and the results compared well with the experimental results for a square building.

1. INTRODUCTION

Distribution of the fluctuating surface pressure and the wind forces acting on bluff-shaped bodies are of great practical interest in the field of structural design in wind engineering. Any increase in building height increases the effect of wind loading. Wind loads on tall structures cause concerns about the integrity of the structure envelope and safety of the whole structural system. Under the influence of the dynamic wind loads, typical high-rise buildings vibrate in the alongwind, acrosswind, and torsional directions. Modern high-rise buildings designed to satisfy static lateral drift requirements still might oscillate excessively during windstorms. The level of these oscillations may be significant enough to cause discomfort to the occupants. An assessment of building motion is an essential prerequisite for serviceability. Extreme loading conditions resulting from severe dynamic wind conditions are needed for the strength design to ensure structural integrity.

Rigorous simulation of the wind flow over a building on a computer is an ambitious undertaking. It requires the numerical solution of the three-dimensional (3-D) Navier–Stokes equations for the full-field flow at high Reynolds number around a bluff body. Some attempt must be made to represent the velocity profile of the incident wind. In general, the flow will be unsteady in time with separation, re-circulation and re-attachment and the flow will be particularly sensitive to conditions in the highly complex flow regime occurring at points of flow separation.

0022-460X/02/$35.00

Many investigations have been conducted in attempts to measure and predict wind loads on structures either by full-scale measurements or by model studies. Generally, wind tunnel tests are conducted to simulate the natural wind flow; however, with the advent of larger and more powerful computer systems, numerical simulation of natural wind flow has gradually gained popularity.

In the past few decades, an increased knowledge of the wind environment, the use of boundary layer wind tunnels, and the development of random vibration theory has resulted in improved analytical and experimental methods for predicting the response of tall buildings. The analytical technique used to predict the alongwind response was developed by Davenport [1] where he introduced the gust factor approach to study the extreme structural response. The concept was later refined by Simiu and Loizer [2] taking into account higher modes of vibration and non-perfect correlation of wind pressures on the windward and leeward walls of the building. More analytical works for alongwind response were presented by Solari [3] and Simiu [4].

The vortex shedding characteristics of square cylinder and associate surface pressure in either smooth or turbulent flows have been under extensive study in the past few decades. Reinhold [5] used a direct pressure measurement technique to determine mean and dynamic forces on a rigid square building model. Tallin and Ellingwood [6], Kareem [7], and Islam *et al.* [8] further utilized pressure measurement results of wind loads to analyze wind-induced lateral–torsional motion of tall buildings. Kareem [7] suggested that for a square-section building, the torsional loads were dominated by the unsymmetrical nature of the acrosswind load fluctuations and less dependent on the alongwind load fluctuations.

The flows around two-dimensional (2-D) cross-section bluff-bodies have been studied in wind tunnels ever since the 1960s (e.g. references [9–12]). Numerical simulations of these flows have also been reported by several authors. Davis and Moore [13] presented a 2-D vortex shedding process from rectangular prisms and compared their results with experimental data. They found that the Strouhal numbers were in good agreement with experiments for Reynolds number less than 1000. Franke and Rodi [14] and Przulj and Younis [15] studied high Reynolds number flows over square prisms using the k–ε model and the Reynolds stress equation (RES) model. Murakami and Mochida [16] conducted both 2- and 3-D simulations using the k–ε method and the LES method for Reynolds number close to 10^5.

In this study, computational fluid dynamics is used to predict the fluctuating wind loads on the building surface. The fidelity of CFD solutions for turbulent flows is dictated by turbulence modelling, because of the complex feature of the flows, especially when it comes to the flows around buildings and structures. One of the challenging features of the flows is that the flows hardly remain at or near equilibrium. The flows around and in the near-wakes of buildings and structures keep changing relentlessly. It is this non-equilibrium nature of the flows that makes turbulence modelling for bluff-body flows difficult.

In spite of the fact that a turbulent flow is intrinsically 3-D, it is still worthwhile to explore the feasibility of a 2-D approximation of a turbulent flow as the means for engineering applications. For a complex engineering problem, it is reasonable to investigate the problem by a 2-D method at preliminary design stage, considering limited available computer resources, before a 3-D approach is attempted for final design. The discrepancies between the 3- and the 2-D models are due to the lack of proper correlation of the forces along the height of the building. For the correct measurement of the correlation, 3-D simulation is needed which is, however, computationally prohibitive. Kwok [17] proposed a design procedure based on modal analysis and random vibration theory. He stated that for the limiting cases of ignoring the co-spectral density function, $C_o(z_1, z_2, f)$, for the fluctuating loads in the vertical direction, there will be a $\pm 16\%$ variation on the force spectra

representing about $\pm 8\%$ variation on the displacement spectra. For tall, slender buildings in turbulent boundary layer flows, C_o approaches 0 is the more likely assumption. In the initial stages of the development of a structure system for a tall building, preliminary estimates of wind loads and the dynamic response associated with the wind motion are required. This study has been directed towards estimating the response of a wind-sensitive building satisfying serviceability requirements facilitating decision making for both the architects and engineers. If necessary, either 3-D analysis or wind tunnel test may be carried out for final design.

2. TURBULENCE MODELS

Virtually all flows of practical engineering interest are turbulent. Turbulent flows are highly random and characterized by fluctuating velocity fields. The extremely small length and time scales involved with turbulent motion require impractical dense computational grids and small time steps when attempting to solve the unaveraged unsteady governing equations for engineering applications at realistic Reynolds numbers. Turbulence modelling is the method of incorporating the critical effects of turbulent motion on the mean unsteady flow having to resolve the actual small scales of turbulent motion. The major challenge of CFD lies in the turbulence modelling.

There are many turbulent models available to deal with turbulent shear flows among which only the Reynolds average Navier–Stokes equations with the k–ε turbulence model and the large eddy simulation (LES) have been widely used for engineering purpose. No single turbulence model is universally accepted as being superior for all classes of problems. The choice of turbulence models depends on considerations such as the physics of the flow, the established practice for a specific class of problem, the level of accuracy required, the available computational resources, and the amount of time available for the simulation. To make the most appropriate choice of model for any application, we need to understand the capabilities and limitations of the various options. The turbulence model will be discussed in the following sections. Detailed information about the turbulence model is given in references [18–20].

2.1. RNG k–ε MODEL

This model is the most widely applied to engineering problems. In the RNG model, the fluctuating velocity field is assumed to be governed by the Navier–Stokes equations driven by a random force. The dynamic equations for the large-scale field are obtained by averaging over an infinitesimal band of smaller scales to remove the latter from consideration. The removal of the smallest scales leads to sub-grid scale models, which can be used in large eddy simulations, while the removal of successively large scales produces Reynolds stress models. The RNG version of the k–ε model contains no undetermined constants, these being calculated explicitly from theory, and does not require wall functions either. The model has much more anisotropy and the related structure built in it when compared with the conventional k–ε model.

2.2. LES MODEL

By large eddy simulation, the large-scale field is calculated directly from the solution of the filtered time-dependent Navier–Stokes equations and the smaller, subgrid scales are

modelled. The large scales are strongly dependent on the flow geometry and therefore LES is capable of predicting them. The model for the subgrid scales then represents the effect of the small scales on the large-scale motion. It is believed that small scales are more universal in character for different flows than large scales. The Smagorinsky–Lilly model proposed by Smagorinsky [21] and further developed by Lilly [22] is adopted for sub-grid scale model in the present study. The Smagorinsky constant $C_s = 0{\cdot}1$ has been found to yield the best results for a wide range of flows, and is the default value in FLUENT 5.

It is theoretically possible to directly resolve the whole spectrum of turbulent scales using an approach known as direct numerical simulation (DNS) which is, however, not feasible for practical engineering problems as the mesh sizes are computationally prohibitive for high Reynolds numbers. The use of LES is a good choice for investigating flows that are too complex to be computed economically by DNS.

3. SIMULATION OF TURBULENT FLOW

Wind speed over a given time interval can be thought of as having a time-invariant mean component,

$$U(z, t) = \bar{U}(z) + u(z, t). \tag{1}$$

The mean wind speed $\bar{U}(z)$ varies with height and terrain roughness and, for engineering purposes, follows a power law or a logarithmic law [23]. The term $u(z, t)$ in the above equation considered as a random process having a mean equal to zero and a mean square σ_u^2 that equals area under the gust power spectrum curve. The power spectrum or power spectral density (PSD) of the fluctuating component of wind speed represents the distribution of turbulent energy in wind as a function of frequency.

A number of methods for simulating stationary random fields with specific spectral density have been discussed by Iannuzzi and Spinelli [24]. The weighted amplitude wave superposition (WAWS) method is adopted in this study. The gustiness of wind has been simulated as a one-variate, one-dimensional homogeneous, Gaussian random process with a zero mean and a spectral density function $S_u(n)$ by the following expression [25]:

$$u(t) = \sqrt{2} \sum_{k=1}^{N} A_k \cos(2\pi n'_k + \varphi_k), \tag{2}$$

where $A_k = \sqrt{S_u(n_k)\Delta n}$, $\Delta n = (n_u - n_1)/N$, $n_u =$ upper frequency limit (Hz), $n_1 =$ lower frequency limit (Hz), $N =$ total number of frequency intervals, $n'_k = n_k + \delta n$, $n_k = n_1 + (k - 0{\cdot}5)\Delta n$, $k = 1, 2, \ldots, N$; δn – a random frequency distributed $-\beta\Delta n/2$ to $\beta\Delta n/2$, $\beta =$ amount of jitter and $\varphi_k =$ a random phase angle, uniformly distributed from 0 to 2π.

Apart from these parameters, the velocity sampling time interval Δt and the total length of the time series T to be simulated are selected based on the desired characteristics of the time series to be generated. To prevent aliasing, the highest frequency n_u in the equivalent wind spectrum is kept less than half the velocity sampling rate $(1/2\Delta t)$ [26].

$$n_u \leqslant (1/2\Delta t).$$

Jitter β is applied to generate non-repeating time series. However, the addition of jitter degrades the performance of the method [27]. Hence, no jitter is added and therefore, $\beta = 0$; $\delta n = 0$. Thus, $n'_k = n_k$. In order to produce a non-repeating or aperiodic equivalent velocity

series, the condition that the total number of frequency intervals is greater than or equal to the total number of sampling intervals in the series, as suggested in reference [27], is adopted. The random phase angles ϕ_k $(k = 1, 2, \ldots, N)$ are generated from uniform distribution in the interval $(0, 2\pi)$, by multiplicative congruential method with constant seed numbers.

In this study, Karman's expression for the power spectra of natural wind velocity is chosen as the target of the present turbulence simulation. The one-side power spectrum $S_u(n)$ of horizontal component of wind velocity is expressed as follows:

$$S_u(n) = 4I_u^2 \bar{U} L_u \{1 + 70{\cdot}8(nL_u/\bar{U})^2\}^{-5/6}, \tag{3}$$

in which, n is frequency, $\bar{U}$ is mean velocity and I_u and L_u are, respectively, the turbulence intensity and scale of horizontal component of wind velocity, which are defined as

$$I_u = \sqrt{\frac{\overline{u^2}}{\bar{U}}}, \quad L_u = \bar{U} \int_0^\infty R(\tau)\, \mathrm{d}\tau,$$

where $R(\tau)$ is the autocorrelation coefficient of horizontal component velocity.

The PSD function by the simulated process is compared with the Von Karman PSD function as shown in Figure 1 for I, L_u and $\bar{U}$ of 8·13%, 0·2245 m and 19·5 m/s respectively. The associated wind process is shown in Figure 2. It has been observed that the global shape is similar for both simulated and target PSD function, but simulated spectral amplitude is slightly higher than that of target PSD function. This discrepancy is most likely due to the fact that for simplicity only one random seed has been taken in this simulation.

4. DESCRIPTION OF THE SIMULATION MODEL

In this study, the wind tunnel test conducted by Reinhold [5] has been adopted for the simulation by CFD methods. A square prism with sharp edges was used as a rigid model of the building in the wind tunnel test. The building model illustrated in Figure 3 is a simple square prism and was chosen because it represents a simple geometric shape often

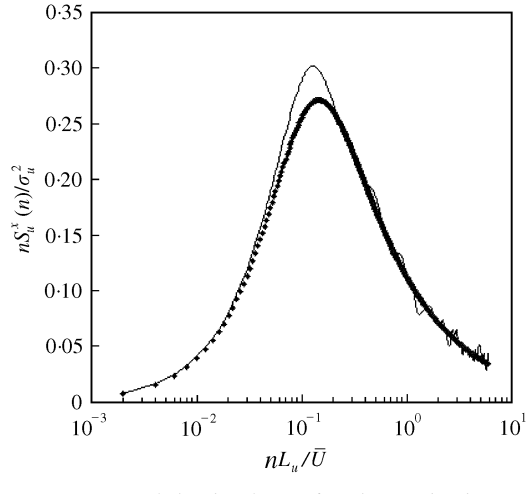

Figure 1. Comparison of Von Karman and simulated PSD functions at level 6: ——, simulation; ♦, Karman.

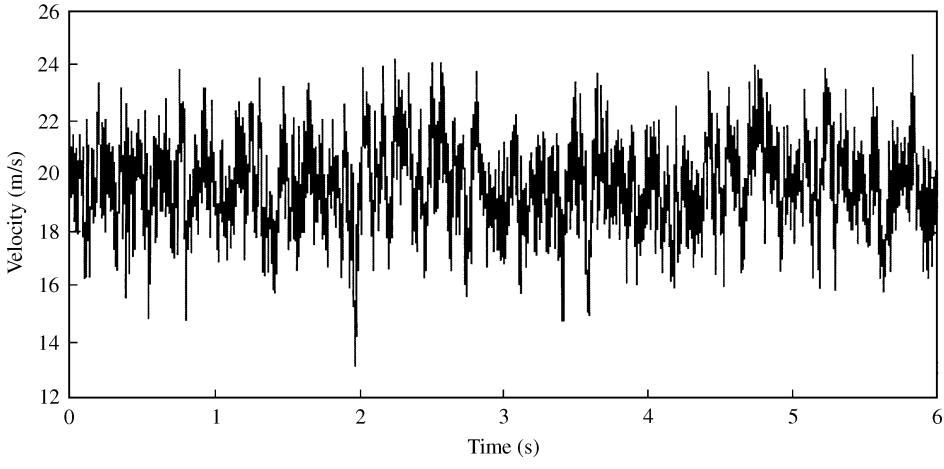

Figure 2. Simulated wind process.

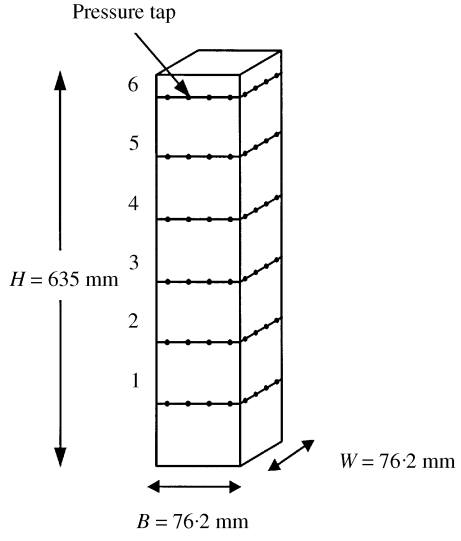

Level	Z (mm)
1	101.6
2	203.2
3	304.8
4	406.4
5	508.0
6	609.6

Figure 3. Wind tunnel model.

encountered in tall buildings. Reinhold attempted to simulate strong winds over urban areas using a method involving the combination of spires and floor roughness. The spires were placed with 600 mm center-to-center spacing at the entrance of the 1·8 m × 1·8 m test-section of the Virginia Polytechnic Institute and State University low-speed wind tunnel. The model scale was determined from the ratios of turbulence integral length scales L_U of the simulated and design flow. Model scale based on the ratio of the surface roughness length parameters for simulated and design flow was also considered. Heavy emphasis was placed upon modelling the turbulence intensity of the flow along with a favorable comparison between the spectra of the simulated flow and Von Karman equation. The mean wind velocity, turbulent intensity, turbulent scale length and Reynolds number for various levels of the building are listed in Table 1.

A detailed description of the mean and the turbulence components for the wind tunnel shear flow, together with a comparison of the flow properties with those of the atmospheric

TABLE 1

Elevation and wind conditions at various levels

Level	Elevation (m)	Velocity (m/s)	Turbulent intensity (%)	Turbulent scale length (m)	Reynolds numbers
1	0·1016	10·1	27·71	0·2211	$5{\cdot}9 \times 10^4$
2	0·2032	13·0	23·13	0·2766	$7{\cdot}5 \times 10^4$
3	0·3048	15·1	18·12	0·3048	$8{\cdot}8 \times 10^4$
4	0·4064	16·8	13·69	0·3052	$9{\cdot}8 \times 10^4$
5	0·5080	18·3	10·25	0·2740	$1{\cdot}1 \times 10^5$
6	0·6096	19·5	8·13	0·2345	$1{\cdot}1 \times 10^5$

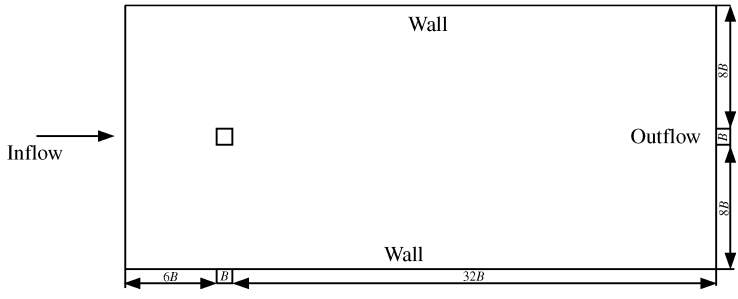

Figure 4. Geometry and boundary condition of the domain.

boundary layer over urban terrain, can be found in reference [5]. The mean velocity profile followed the power law with a power index of 0·37 and the turbulence properties were found to compare reasonably well with full-scale estimates at a geometric scale ratio ranging from 1/400 to 1/600. The model used in the experiment had a height-to-width ratio of 8·3 : 1 and was square in plan. The transducers were located at six elevations throughout the height in layers of 16 about the model perimeter, with four transducers on each side. The Hanning-window function was used to weigh the correlation functions and in the calculations of both power and cross-sepctra to smooth the estimates.

In Reinhold's wind tunnel, pressure was taken for six levels of the building as shown in Figure 3, because it is impractical to set transducer throughout the height of the building. As this study is to simulate the wind tunnel test conducted by Reinhold, six levels' force spectra have been calculated from 2-D simulation. A cylinder with a square section of $76{\cdot}3 \times 76{\cdot}3$ mm has been considered for each level of the building. The height of the model building is 635 mm as shown in Figure 3. Cross-section and the surrounding domain are the same for the six levels, but velocity ($\bar{U}$), turbulent intensity (I) and turbulent scale length (L_u) vary for different levels as shown in Table 1.

The domain of the simulation is described in Figure 4. The domain limits are far enough to prevent any influence of boundary conditions, and particularly the exit conditions. The computational domain is $39B$ in the streamwise direction and $17B$ in the cross-stream direction. The square section is located at the center in the lateral direction, and its front face is at a distance of $6B$ from the entrance flow boundary. The calculation is made on 3000 time steps of 0·001 s. The time step chosen is small enough to capture the vortex shedding phenomenon. A quadrilateral mesh with 8000 computational cells as shown in Figure 5 has been adopted for this study. Thirty computational cells have been chosen along each side of

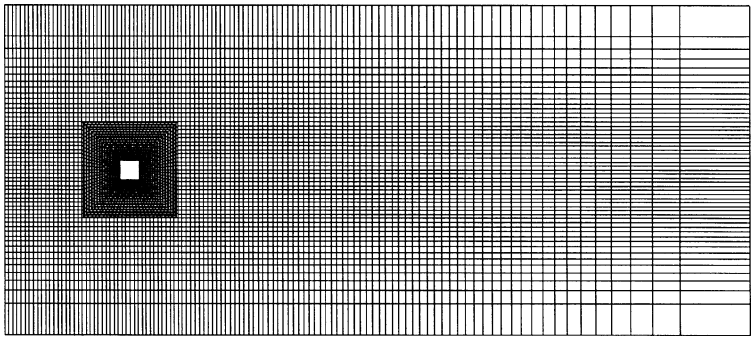

Figure 5. Meshing of the domain.

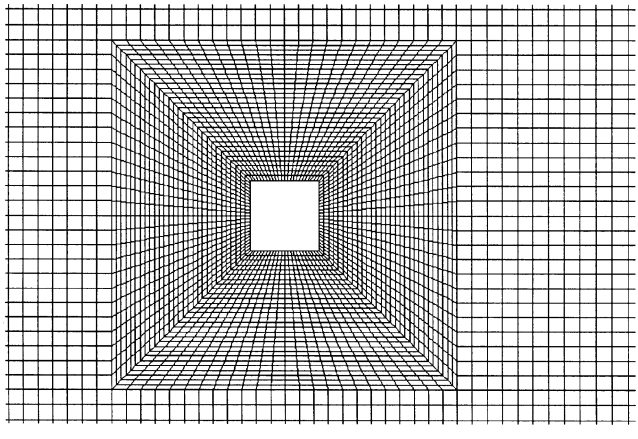

Figure 6. Meshing near the building wall.

the square section, and cell pressures are integrated by FLUENT solver to obtain the forces (N/m) applying onto each face. Figure 6 depicts the mesh near the square section.

For the current study, only wind direction normal to the velocity inlet boundary was used. Outlet boundary and velocity inlet boundary were specified at the sides and wall boundary at the top and bottom of the domain. No-slip boundary conditions are imposed on wall boundary. The inflow boundary conditions were chosen to match the velocity turbulence profiles measured in the wind-tunnel experiments. Outflow boundary conditions were chosen to maintain constant longitudinal rate of change of all dependent variables (i.e., constant slope).

Geometry and mesh have been generated in a package called GEOMESH, which comprises two parts; one is DDN, responsible for geometry construction, and the other is P-CUBE, responsible for mesh generation. Mesh file from GEOMESH is transferred to FLUENT, and the solution procedure and boundary conditions are set. For this study, inlet velocity is random, following the Von Karman spectrum. A user-defined function, written in C language, has been developed to set the inlet boundary condition. The philosophy of FLUENT solver is to run the user-defined function at every iteration. So care should be taken to reduce the time taken by the user-defined function. The user-defined function has been written in such a way that it takes the inlet velocity at every time step from the inlet velocity file generated by the WAWS method, described in section 3, and thus the time consumed by the WAWS method to generate random velocity is avoided in the solver.

5. DYNAMIC RESPONSE OF BUILDING

The equation of motion of a building represented by a discretized lumped-mass system is given by

$$[m]\{\ddot{y}\} + [c]\{\dot{y}\} + [k]\{y\} = \{f(t)\}, \tag{4}$$

in which $[m]$, $[c]$, and $[k]$ are assembled mass, damping and stiffness matrices of the discretized system respectively. In general, the assembly process involves transformation and condensation that reduces the system degree of freedom to the global co-ordinate system consisting of two translations and one rotation per story level. The equation of motion can be solved with various methods. In this study, Galerkin's method is used to solve the coupled equation of motion. Let the assumed set of separable displacement functions be

$$\{y\} = [\phi(z)] \cdot \{q(t)\}, \tag{5}$$

where $[\phi(z)]$ is the shape function of $\{q(t)\}$ the amplitude which is a function of time. Applying the Galerkin technique to equation (4) gives

$$\int_0^H [\phi]^{\mathrm{T}}[[m]\{\ddot{y}\} + [c]\{\dot{y}\} + [k]\{y\}]\,\mathrm{d}z = \int_0^H [\phi]^{\mathrm{T}}\{f(t)\}\,\mathrm{d}z. \tag{6}$$

Integrating by parts and substituting the boundary conditions lead to

$$[M]\{\ddot{q}\} + [C]\{\dot{q}\} + [K]\{q\} = \{F\}, \tag{7}$$

where

$$[M] = \int_0^H \{\phi\}^{\mathrm{T}}[m][\phi]\,\mathrm{d}z, \qquad [C] = c_1[M] + c_2[K], \tag{8, 9}$$

$$[K] = \int_0^H \{\phi\}^{\mathrm{T}}[k][\phi]\,\mathrm{d}z, \qquad \{F\} = \int_0^H \{\phi\}^{\mathrm{T}}\{f(t)\}\,\mathrm{d}z. \tag{10, 11}$$

Proportioning damping matrix is assumed and c_1 and c_2 are constants which can be determined from the specified damping coefficients of two major modes [28].

In the analysis of wind excitation of tall buildings, it is seldom necessary to evaluate and sum the response over more than a few modes. In many cases the first term, corresponding to the fundamental mode of the vibration is quite adequate. A simple linear mode shape, $\phi(z) = z/h$, has been chosen for the present study. Since wind loads are stochastic in nature, the dynamic response of the system can be obtained using a frequency domain approach or a step-by-step time-integration method. The frequency domain approach is adopted in the present study. Following the classical random vibration approach, the relation between the forcing function and response cross-spectral density function is given by

$$[S_q(n)] = [H(n)][S_F(n)][H^*(n)]^{\mathrm{T}}, \tag{12}$$

where $[S_q(n)]$ and $[S_F(n)]$ are the spectral densities of the response and generalized force and $[H(n)]$ and $[H^*(n)]^{\mathrm{T}}$ are the complex frequency transfer function and its conjugate respectively.

$$[H(n)] = [-n^2[M] + in[C] + [K]]^{-1}, \tag{13}$$

$$[S_F(n)] = \begin{bmatrix} S_{F_{xx}} & S_{F_{xy}} & S_{F_{xt}} \\ S_{F_{yx}} & S_{F_{yy}} & S_{F_{yt}} \\ S_{F_{tx}} & S_{F_{ty}} & S_{F_{tt}} \end{bmatrix}, \tag{14}$$

Works by Kareem [29] and Islam [30] suggested that the correlation between the alongwind and acrosswind forces as well as between the alongwind and torque were insignificant. These findings coincided with those reported by Tallin and Ellingwood [6], who pointed out that the correlations were in the order of 0·01 or less in absolute value. Thus, $S_{F_{xy}}$, $S_{F_{yx}}$, $S_{F_{xt}}$ and $S_{F_{tx}}$ are negligible and the spectral density matrix of the force can be written as

$$[S_F(n)] = \begin{bmatrix} S_{F_{xx}} & 0 & 0 \\ 0 & S_{F_{yy}} & S_{F_{yt}} \\ 0 & S_{F_{ty}} & S_{F_{tt}} \end{bmatrix}. \tag{15}$$

The spectral density matrix of the displacement is given by

$$[S_R(n) = [\phi]^{\mathrm{T}}[S_q(n)][\phi]. \tag{16}$$

The matrix of mean square response is given by

$$[\sigma_R^2] = \left[\int_0^\infty [S_R(n)] \, \mathrm{d}n \right]. \tag{17}$$

In this study, all spectral density functions are assumed to be one sided.

6. DETERMINATION OF THE GENERALIZED FORCE SPECTRA

It has been shown [31, 32] that the greatest response occurs when the wind direction is normal to a face of the building. In this study, direction of wind normal to the wall has been considered. The quantitative description of wind loads is based on the assumption that motion of the structure can be neglected when determining the forces acting on it. Thus, the forces measured on a rigid model in this simulation are representative of the forces acting on a full-scale prototype having a similar geometry.

The lift force and torque were found to be strongly correlated. These findings further reinforce the necessity of incorporating the cross-spectrum in the analysis in order to predict the vibration of the structure correctly. However, the response of the structure due to the co-spectra of this statistical coupling may be negligible when the translational and rotational frequencies are reasonably separated. This is attributed to the fact that the cross-modal complex frequency response function $H_i(n)H_j(n)^*$ become negligible compared to the corresponding frequency response functions $|H_j(n)|^2$ and $|H_j(n)|^2$ as the ith and the jth modal frequencies (translational and rotational) become separated [30].

If the loads at different levels are known, the generalized forces associated with any shape functions can be computed by summing up the weighted level forces. These weighting factors take into account the shape function and the tributary area in which the forces are acting. The weighting function is expressed as

$$W_j^{(i)} = (a_j)(\phi_j^{(i)}), \tag{18}$$

where $W_j^{(i)}$ is the weighting factor, a_j is the tributary area associated with level j and $\phi_j^{(i)}$ is the jth level ordinate of the ith shape function. For the linear shape function, $\phi(z) = (z/h)$, adopted in this study, the first term of the weighting function is

$$[W] = \begin{bmatrix} 0{\cdot}0203 \\ 0{\cdot}0325 \\ 0{\cdot}0488 \\ 0{\cdot}0650 \\ 0{\cdot}0813 \\ 0{\cdot}0732 \end{bmatrix}.$$

The value of W at level 6 decreases from 0·0813 to 0·0732 due to the reduction in the tributary area at the top.

The generalized force spectrum matrix can thus be expressed as

$$[S_F(n)] = \begin{bmatrix} W^{\mathrm{T}} S_{P_{xx}} W & W^{\mathrm{T}} S_{P_{xy}} W & W^{\mathrm{T}} S_{P_{xt}} W \\ W^{\mathrm{T}} S_{P_{yx}} W & W^{\mathrm{T}} S_{P_{yy}} W & W^{\mathrm{T}} S_{P_{yt}} W \\ W^{\mathrm{T}} S_{P_{tx}} W & W^{\mathrm{T}} S_{P_{ty}} W & W^{\mathrm{T}} S_{P_{tt}} W \end{bmatrix}. \tag{19}$$

The generalized force spectrum matrix has to be described in dimensionless form before it can be applied to a full-scale prototype building of similar geometry. Several normalizing schemes may be used for this purpose. They are (1) normalization with respect to the mean square value of the forces and (2) normalization with respect to the mean dynamic wind pressure at the top of the building. The former is adopted in the present study.

7. RESULTS AND DISCUSSION

The computations were carried out with 8000 computational cells on the computer facilities of Supercomputing & Visualisation Unit at the National University of Singapore. A single time step takes 0·37 mins of CPU time on SGI Origin2000 machine.

Across-wind force is critical due to its vortex nature and there is no analytical method to calculate across-wind and torsional responses of a building. In wind tunnel, large number of pressure transducers and analog circuits are used to determine fluctuating wind loads for various levels of the building. In this study, each level of the building is considered as a 2-D model. Both the LES and RNG k–ε methods are used to simulate the random flow around a square cylinder which is equivalent to a level of the building. A second order accurate temporal discretization scheme is used along with a second order upwind for convection term.

For uniform flow, with 8000 computational cells and Re ($= 8 \times 10^4$), the RNG k–ε method gives the value of 0·134 for Strouhal number which agrees well with the experimental result presented by Lyn [33]. But when the input flow is random, RNG k–ε cannot capture the high fluctuation of pressure, i.e., it does not give the required vortex shedding phenomenon accurately. On the other hand, the LES method, with the Smagorinsky model as a sub-grid model, is able to predict vortex shedding nature for random velocity input. Figures 7–9 show the streamline at various time steps of level 6. The shedding motion is well produced, with a vortex shed from the lower side of the cylinder, which makes the flow complex. It is also visible from these figures that outflow boundary

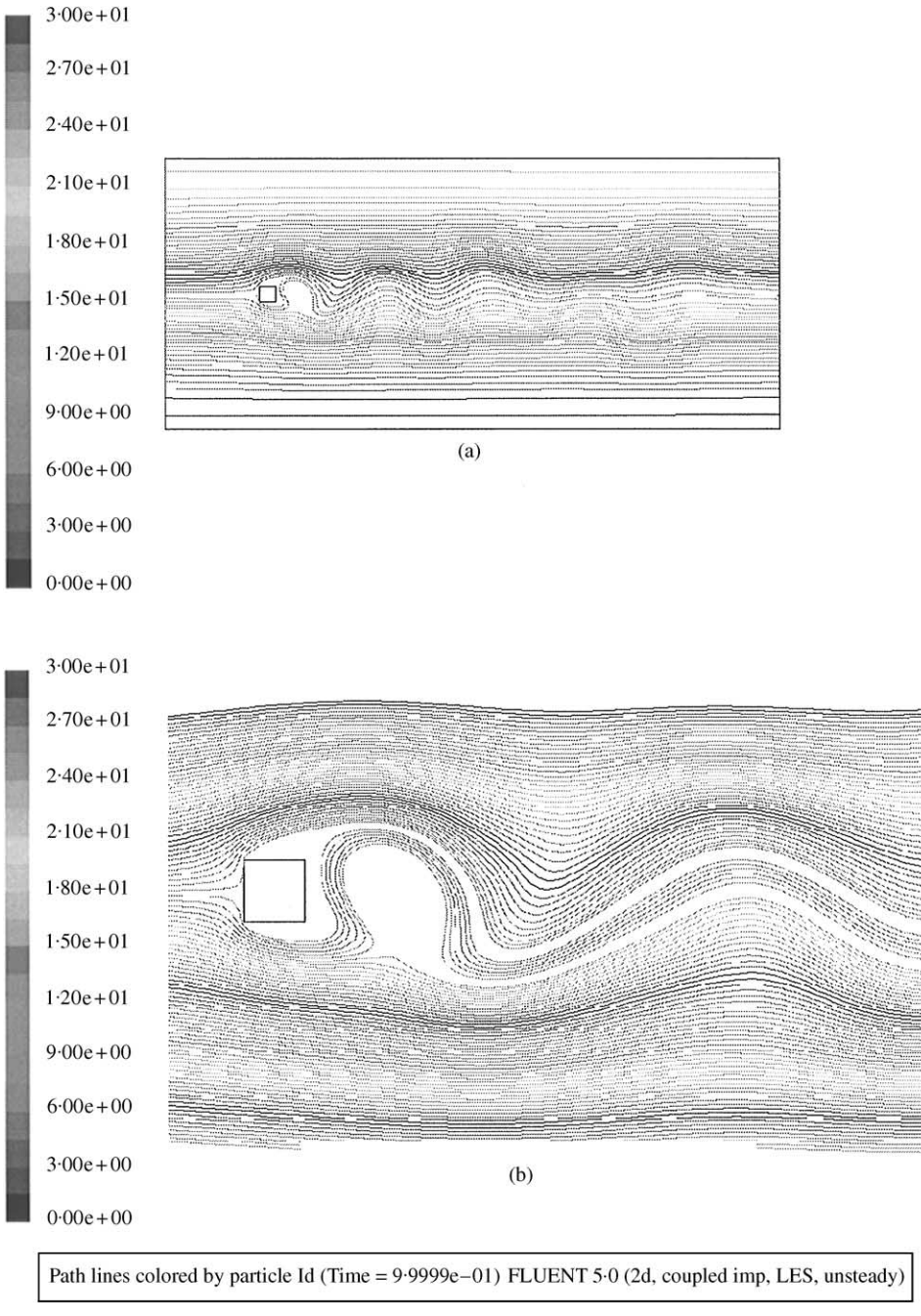

Figure 7. Streamline at the 1000th time step (level 6): (a) entire domain; (b) streamline near the obstacle.

has been chosen far away from the cylinder so that the outflow boundary does not affect vortex shedding motion.

As our main interest is in the response of the building due to the random wind velocity, we need to get the force acting on the side wall of the building at every level. Each level of Reinhold's [5] model, where transducers were located, has been simulated as a 2-D model.

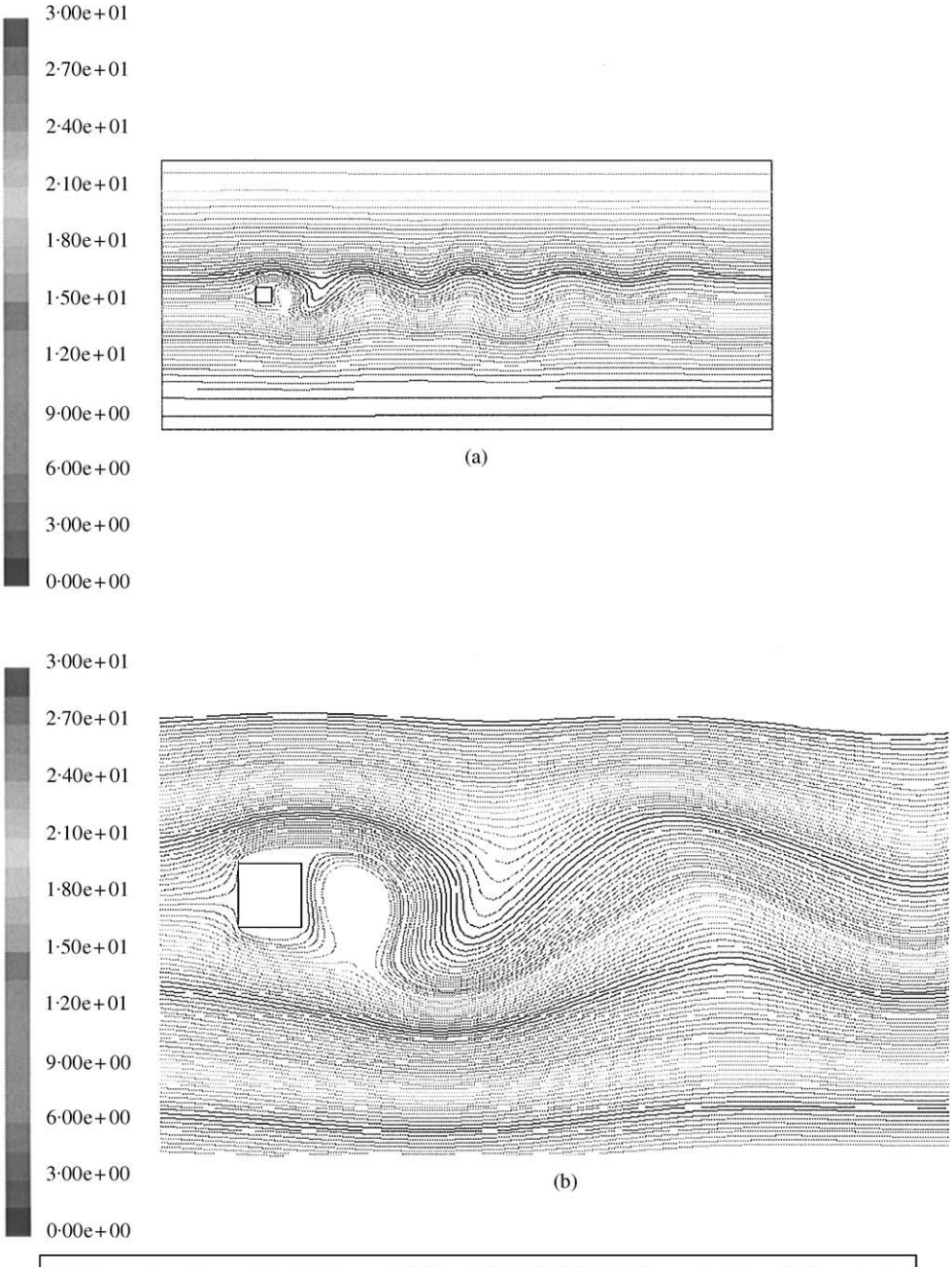

Figure 8. Streamline at the 2000th time step (level 6): (a) entire domain; (b) streamline near the obstacle.

Wind force spectrum has been developed for each level of the building as described in section 4.4. Matlab signal processing toolbox has been used for spectral analysis, and spectral densities of forces are generalized with their mean values. Figures 10–12 show the normalized power spectral density of the alongwind (drag) forces, acrosswind (lift) forces and torsional moments, respectively, using the LES model.

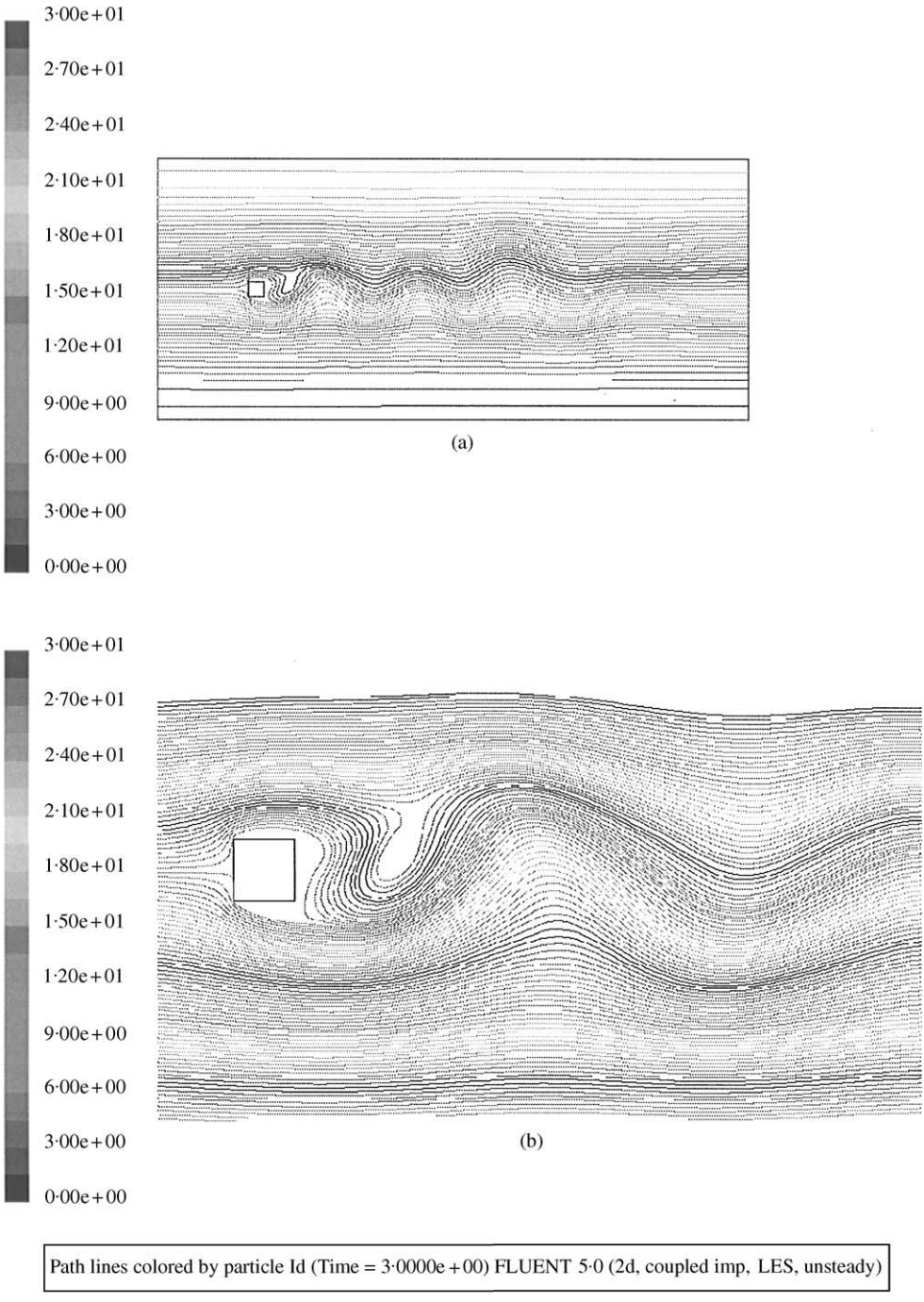

Figure 9. Streamline at the 3000th time step (level 6): (a) entire domain; (b) streamline near the obstacle.

The normalized power spectra for the alongwind force components are typical of random loading and show good agreement with experimental results by Reinhold [5]. For each level, simulating vortex shedding frequency is in good agreement with experimental value. But as the height decreases, the frequencies at which peaks occur shift to the left. This is due

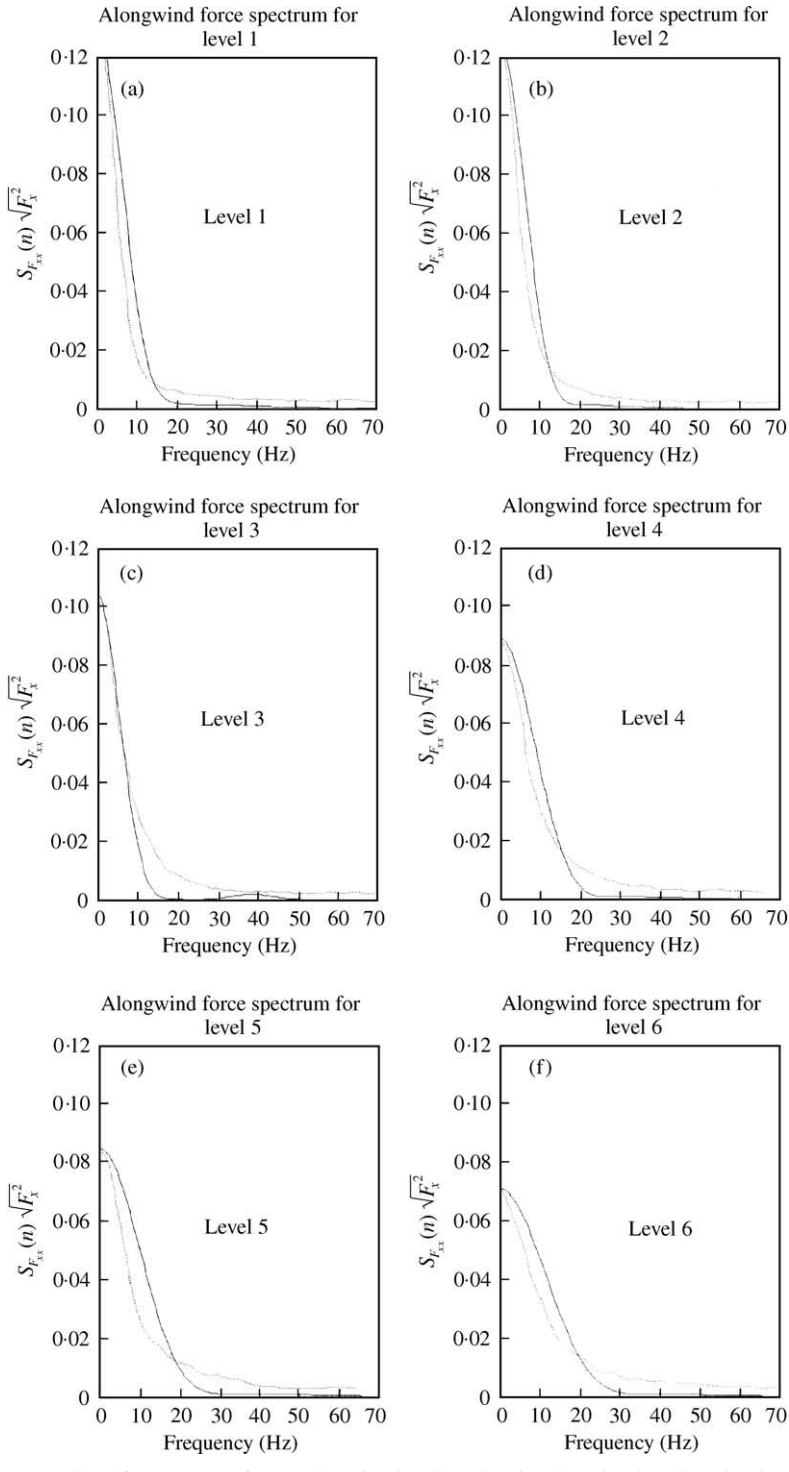

Figure 10. Normalized force spectra for F_x: (a) at level 1; (b) at level 2; (c) at level 3; (d) at level 4; (e) at level 5; (f) at level 6: ——, simulation; ·····, experiment.

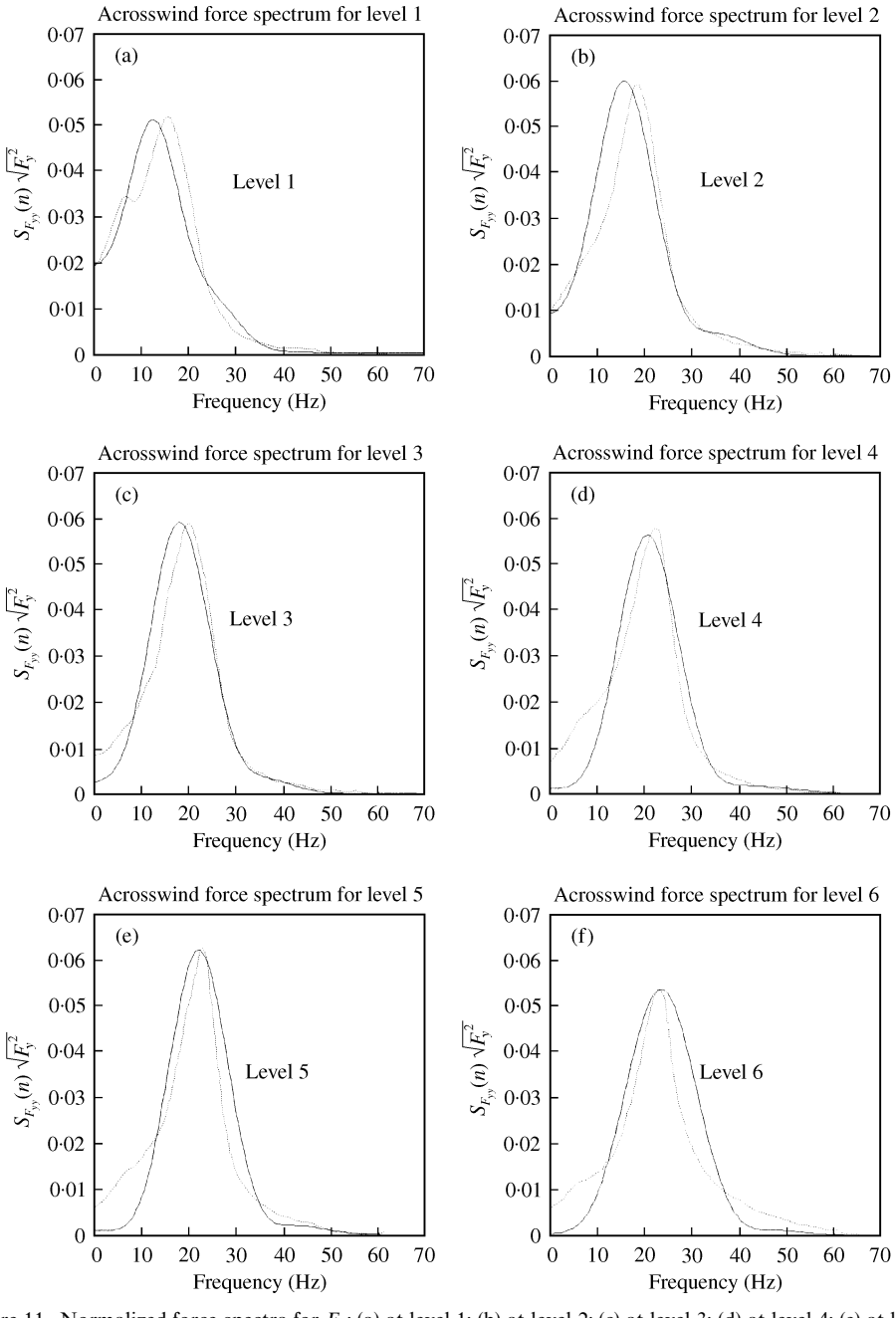

Figure 11. Normalized force spectra for F_y: (a) at level 1; (b) at level 2; (c) at level 3; (d) at level 4; (e) at level 5; (f) at level 6: ——, simulation; ·····, experiment.

to the fact that with the decrease in height, turbulence intensity increases. For the present study, moment spectra show similarity with the acrosswind spectra, i.e., concentrated excitation energy for moment is associated with the vortex shedding process. However, experimental moment spectra show moderate concentration of energy over a wide range of frequencies. Kareem [7] has shown that the torsional loads are dominated by the

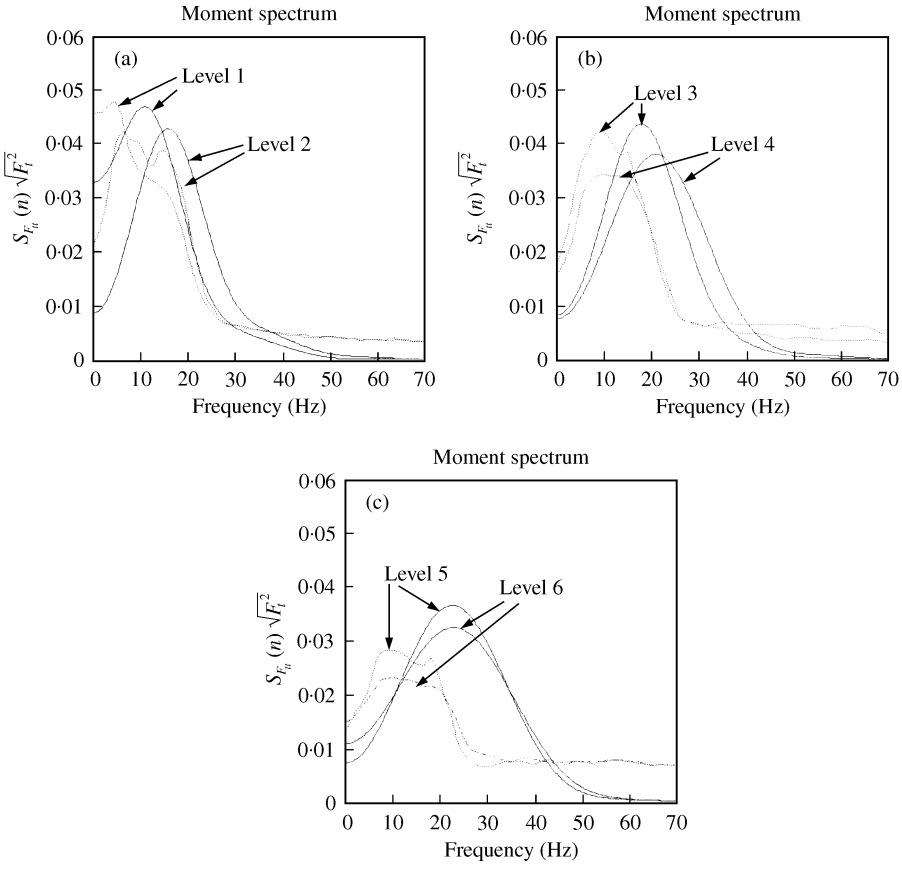

Figure 12. Normalized force spectra for F_t: (a) at levels 1 and 2; (b) at levels 2 and 3; (c) at levels 5 and 6: ——, simulation; ·····, experiment.

unsymmetrical nature of the acrosswind load fluctuations and are less dependent on the alongwind load fluctuations for a square cross-section building implying that the dominant part responsible for the torque is mainly due to the randomness of the acrosswind force which agrees well with results from the present study. Details of the similarity of normalized reduced modal spectra of the wind forces of the present study compared with those of Kareem [7] are presented in reference [34].

A 180 m × 30 m × 30 m building having a density of 190·0 kg/m^3 and a damping ratio of 0·01 studied earlier by Islam [30] based on the fluctuating wind forces obtained from the wind tunnel test carried out by Reinhold [5] is reanalyzed for r.m.s. accelerations in alongwind, acrosswind and torsional directions. Only the first term of the polynomial function, z/H is used to span the displacement field. The building is subjected to wind load with velocity at the top, $\bar{U}(h) = 28$ m/s. The fundamental frequencies of the building are 0·2, 0·2 and 0·235 Hz for alongwind, acrosswind and torsional directions respectively. R.m.s. accelerations using the above normalized force spectra are shown in Table 2. Alongwind and acrosswind accelerations show fairly good agreement with results by Islam [30]. R.m.s. acceleration for torsion, however, deviates somewhat from Islam's value as he adopted the moment spectra from experimental study which differ substantially in shape from the moment spectra obtained in the present study as described earlier.

TABLE 2

Comparison of r.m.s. accelerations

	r.m.s. acceleration		
	σ_u ($\times 10^{-2}$ m/s^2)	σ_v ($\times 10^{-2}$ m/s^2)	σ_t ($\times 10^{-3}$ rad/s^2)
Islam's work	4·066	7·341	2·95
Present study	4·2	7·85	1·3

8. CONCLUSION

The primary purposes of this study are to establish (1) the acrosswind force and torsional spectra for time-dependent turbulent flows with large-scale unsteadiness and turbulence using CFD and (2) the response of a building under fluctuating wind load. A linear fundamental mode was used to derive modal generalized force spectra. For wind direction normal to the building, vortex shedding is the dominant mechanism of torsional excitation. A computer program was developed to evaluate the dynamic response of the building in frequency domain.

The simulation procedure presented in this study provides a complete estimation from the generation of turbulent wind to the estimation of r.m.s. response of the wind-induced vibration of a building, which can be used in lieu of wind tunnel studies. It can be concluded from the present study that (1) the LES model plays an important role in dealing with turbulent modelling issues that the RNG k–ε model cannot resolve and (2) the 2-D model can predict the response of the building with sufficient accuracy for preliminary design purposes. Although the requirements in computing resources for LES are higher than those for the RNG k–ε model they are still much lower than those needed for DNS. Recent advances in computer technology made it possible that LES can be used for general engineering purpose as a reliable design tool for setting turbulent models.

The computer modelling technique may eventually enhance the design process of buildings and structures against wind loading. This will complement the current design practice of using building codes and standards or performing experiments in wind tunnels. Experiments and computer modelling can be used to supplement each other in identifying the critical parameters of wind effects on buildings. In the earlier stage of design computer modelling approach can be used as a predictive tool to obtain a wider range of design alternatives at reduced cost. This study permits the building response to be estimated at the preliminary design stages with less effort. This would allow early assessment of the serviceability requirement to reduce the acceleration level at the top floors to ensure occupancy comfort. This estimate will also assist the designer to assess the need for a more exact investigation by a boundary-layer wind tunnel test. The correct measurement of correlation of forces along the vertical direction can be obtained, if required, through 3-D analysis.

REFERENCES

1. A. G. DAVENPORT 1967 *Journal of the Structural Division, American Society of Civil Engineers* **93**, 11–344. Gust loading factors.
2. E. SIMIU and D. W. LOIZER 1975 *National Bureau of Standards Science Series* **74**. *Washington, D.C.: U.S. Government Printing Office*. The buffeting of tall structures by strong winds.

3. G. SOLARI 1983 *Journal of Wind Engineering and Industrial Aerodynamics* **14**, 467–478. Analytical estimation of the alongwind response of structures.
4. E. SIMIU 1980 *Journal of Structural Engineering*, *American Society of Civil Engineers* **106**, 1–10. Revised procedure for estimating along-wind response.
5. T. A. REINHOLD 1977 *Ph.D. Thesis*, *Virginia Polytechnic Institute & State University*, *U.S.A.* Measurement of simultaneous fluctuating loads at multiple levels on a tall building in a simulated urban boundary layer.
6. A. TALLIN and B. ELLINGWOOD 1985 *Journal of Structural Engineering*, *American Society of Civil Engineers* **111**, 2197–2213. Wind induced lateral–torsional motion of buildings.
7. A. KAREEM 1985 *Journal of Structural Engineering*, *American Society of Civil Engineers* **111**, 2479–2496. Lateral torsional motion of tall buildings to wind loads.
8. M. S. ISLAM, B. ELLINGWOOD and R. B. COROTIS 1999 *Journal of Wind Engineering and Industrial Aerodynamics* **116**, 2982–3002. Dynamic response of tall buildings to stochastic wind loads.
9. B. J. VICKERY 1966 *Journal of Fluid Mechanics* **125**, 481–494. Fluctuating lift and drag on a long cylinder of square cross-section in a smooth and in a turbulent stream.
10. B. E. LEE 1975 *Journal of Fluid Mechanics* **69**, 263–282. The effects of turbulence on the surface pressure field of a square prism.
11. T. MIYATA and M. MIYAZAKI 1979 *Wind Engineering Proceedings*: *Fifth International Conference*, *Fort Collins*, *CO*, *U.S.A.* 631–642. Turbulence effects on aerodynamic response of rectangular bluff cylinders.
12. P. W. BEARMAN and E. D. OBASAJU 1982 *Journal of Fluid Mechanics* **119**, 297–321. An experimental study of pressure fluctuations on fixed and oscillation square-section cylinders.
13. R. W. DAVIS and E. F. MOORE 1982 *Journal of Fluid Mechanics* **116**, 475–506. A numerical study of vortex shedding from rectangles.
14. R. FRANKE and W. RODI 1991 *Proceedings of Eighth Symposium on Turbulent Shear Flows*, 189. Calculation of vortex shedding past a square cylinder with various turbulence models.
15. V. PRZULJ and B. A. YOUNIS 1993 *American Society of Mechanical Engineering*, *Fluid Engineering Division* **149**, 75. Some aspects of the prediction of turbulent vortex shedding from bluff bodies.
16. S. MURAKAMI and A. MOCHIDA 1995 *Journal of Wind Engineering and Industrial Aerodynamics* **54**, 191–211. On turbulent vortex shedding flow past a square cylinder predicted by CFD.
17. K. C. K. KWOK 1982 *Engineering Structures* **4**, 256–262. Cross-wind response of tall buildings.
18. V. YAKHOT and S. A. ORSZAG 1986 *Journal of Scientific Computing* **1**, 1–15. Renormalization group analysis of turbulence.
19. B. A. GALPERIN and S. A. ORSZAG 1993 *Large Eddy Simulation of Complex Engineering and Geophysical Flows*. Cambridge: Cambridge University Press.
20. Fluent User Guide: Vol. 1–4. Fluent Inc. August 3, 1998.
21. J. SMAGORINSKY 1963 *Monthly Weather Review* **91**, 99–164. General circulation experiments with the primitive equations. I.: The basic experiment.
22. D. K. LILLY 1966 *NCAR Manuscript* 123. On the application of the eddy viscosity concept in the internal subrange of turbulence.
23. E. SIMIU and R. H. SCANLAN 1996 *Wind Effects on Structures*: *Fundamental and Applications to Design*. New York: John Wiley.
24. A. IANNUZZI and P. SPINELLI 1987 *Journal of Structural Engineers American Society of Civil Engineers*, **113**, 2382–2398. Artificial wind generation and structural response.
25. M. SHINOZUKA and C. M. JAN 1972 *Journal of Sound and Vibration* **25**, 111–128. Digital simulation of random process and its applications.
26. A. V. OPPENHEIM, A. S. WILLSKY and I. T. YOUNG 1983 *Signals and System*. Englewood Cliffs, NJ: Prentice-Hall. Signal processing series.
27. W. O. JEFFRIES, D. G. INFIELD and J. MANWELL 1991 *Journal of Wing Engineering* **15**, 147–154. Limitations and recommendations regarding the shinozuka method for simulating wind data.
28. R. R. CRAIG 1981 *Structural Dynamic*: *An Introduction to Computer Methods*. New York: John Wiley & Sons.
29. A. KAREEM 1978 *Ph.D. Thesis*, *Colorado State University*. Wind excited motion of buildings.
30. M. S. ISLAM 1988 *Ph.D. Thesis*, *The John Hopkins University*. Modal coupling and wind-induced vibration of tall buidlings.
31. A. TALLIN 1984 *Ph.D. Thesis*, *The John Hopkins University*. Wind induced motion of tall buildings.

32. T. A. REINHOLD and P. R. SPARKS 1980 *Proceedings of Fifth Conference on Wind Engineering, Fort Collins, CO*. The influence of wind direction on the response of a square-section tall building.
33. D. A. LYN 1989 *Proceedings of* 23*rd Congress, International Association for Hydraulic Research, Ottawa, Canada*, 21–25. A85–A92. Phase-averaged turbulence measurements in the separated shear layer region of flow around a square cylinder.
34. M. S. KHAN 2000 *M.Eng. Thesis, National University of Singapore*. Dynamic response of wind-excited tall buildings using CFD.

APPENDIX A: NOMENCLATURE

b	breadth of structure
c_1, c_2	damping coefficients
I_u	longitudinal velocity turbulent intensity
$\bar{F}_x^2$	mean square force in x direction
$\bar{F}_y^2$	mean square force in y direction
F_t^2	mean square of torsional moment
k–ε	turbulent kinetic energy dissipation model
L_u	longitudinal turbulent scale length, m
$S_{F_{xx}}, S_{F_{yy}}, S_{F_{tt}}$	generalized drag, lift and torsion spectra
$S_{P_{xx}}, S_{P_{yy}}$	drag and lift pressure spectra
U	total wind velocity
$\bar{U}$	mean wind velocity
W	weighting function
Δt	time step
Δn	frequency step
β	amount of jitter to produce an aperiodic time series
ω_k	random phase angle
δ_n	uniformly distributed random frequency
ϕ	displacement shape function
σ_R	r.m.s. displacement response
CFD	computational fluid dynamics
LES	large eddy simulation
RNG	renormalization group theory